Developing a low-fluid pressure safety valve design through a numerical analysis approach

T. Barbaryan

School of Mechanical Engineering, University of Birmingham, Birmingham, UK

S. Hoseinzadeh*

Department of Mechanical and Aeronautical Engineering,
Centre for Asset Integrity Management, University of Pretoria, Pretoria, South Africa and Young Researchers and Elite Club, West Tehran Branch, Islamic Azad University, Tehran, Iran

P.S. Heyns

Department of Mechanical and Aeronautical Engineering,
Centre for Asset Integrity Management, University of Pretoria, Pretoria, South Africa, and

M.S. Barbaryan

Department of Mechanical Engineering, Islamic Azad University, Tehran, Iran

*Corresponding author
S. Hoseinzadeh can be contacted at: hoseinzadeh.siamak@gmail.com

Abstract

Purpose – This study aims to develop a new design for the fluid-safety valve to make it more environmentally friendly.

Design/methodology/approach – Computational fluid dynamics is carried out to analyse the behaviour of flow in both traditional and new safety valves.

Findings – The possibility of failure in the new design under the maximum allowable working pressure is analysed using finite element analysis.

Originality/value – Investigating a new low-fluid pressure safety valve design.

Keywords Pressure relief valve, Weight loaded safety valve,
Maximum allowable working pressure, Finite element analysis, Computational fluid dynamics

Paper type Research paper

1. Introduction

Safety is the number one priority in most industries, and more so in process plants, as minor mistakes can lead to catastrophic explosions, which can cause fatalities and loss of valuable resources such as oil and gas (Srivastava and Gupta, 2010; Baladeh *et al.*, 2019). One of these precautions is the installation of safety relief valves where the maximum allowable working pressure is likely to be exceeded (Hellemans, 2011; Mitchell *et al.*, 2013). According to the British Standards Institution (BS EN ISO 4126-1:2004), a safety valve is described as a device that opens when the fluid pressure inside the vessel becomes greater than a predetermined set pressure and closes when a volume of excess pressure is released, so that

the valve disc returns on the seat (Kale, 2014). There are several types of pressure relief valves such as weight loaded, spring loaded, pilot operated and metal rupture disc safety valves (BS EN ISO 4126-1, 2004; Bukowski *et al.*, 2014).

Bursting (or rupture discs) is another type of safety valve, which is torn in the event of an overpressure situation to relieve the excess pressure. It is a non-reclosing valve and can be used when the fluid is not toxic and not considered valuable (Wang *et al.*, 2012).

Pilot operated safety valves are used in more complex systems and consists of two main parts, namely, the pilot and the piston. The pilot itself is a spring loaded safety valve of smaller dimensions. Therefore, it cannot release the excess pressure but it is used to trigger the pressure relief process via the piston. Fluid is in direct contact with the bottom surface of the piston, which has a smaller area. Moreover, the pilot is in contact with both the bottom and top sides of the piston via a pipe. As the area of the top of the piston is larger than the bottom, it is exposed to more fluid, so the valve will remain closed. However, when the fluid reaches a set pressure, the pilot that is a direct acting safety valve starts to relieve the excessive pressure and this causes a lower force on the larger area of the piston and opens the valve (Chung *et al.*, 2000; Hos *et al.*, 2014).

Direct acting safety valves such as weight and spring loaded safety valves operate only by the force caused by fluid pressure. Before they open, the fluid pressure is opposed by the weight or spring pressure on the disc and when this pressure becomes greater, the gate will open. Also, the displacement of the disc depends on the amount of fluid pressure but when the build-up pressure is released, this force will cause the disc to close and prevent the fluid to escape (Ye and Chen, 2009; Dasgupta and Karmakar, 2002).

Weight loaded safety valves usually use lead as their weight material. Lead is classified amongst the highly toxic materials. There are also fairly limited resources of lead left in the world, which compels engineers to explore replacement materials. However, the problem is not as simple as it may sound. Lead is among the densest metals by having a density of 11,000 (kg/m^3). Having a relatively low price makes it a unique choice for engineers to select lead as preferred material in weight based mechanisms.

This research is considered a weight loaded safety relief valve manufactured by Elmac Technologies (2011), which uses lead as its weight material. However, due to the problems with lead, it has to be replaced with other materials, which make it a tougher challenge for the designers, as any other material within the same price range has a relatively lower density that would increase the weight dimensions to have the same weight effect.

2. Definition and design of problem

2.1 The original design

The product considered here is a "pressure relief valve to atmosphere", which has a maximum set pressure of 80 mbar and can be adjusted to work with lower set pressures by using smaller weights (Elmac technologies, 2011). This product is used on the top of a natural gas vessel and is attached to the vessel using a flange connection at the bottom of the safety valve. This type of safety valve has a flame arrester installed on top of the valve body, which is protected by a hood that covers the weight from above. Flame arresters play an important role in safety regulations. Their function is to prevent fire entering into the vessel in case the relieved gas explodes. The hood also works as a filter, which prevents dust particles to enter the valve, as well as protects the safety valve from direct sunlight and extreme weather.

On the valve body, a pallet with a lead weight on top of it is adjusted to close the valve. An O-ring is used between the valve body and the pallet to prevent leakage of fluid and seal it. Therefore, when the pressure of the bulk storage tank is below the set pressure, the total

weight of the pallet and the lead weight will push the O-ring into its place to seal the valve completely.

In Figure 1 three rods can be seen. These three rod are pressure guide rods that control the movement of the pallet by making it move along the Y-axis. One of these pressure guide rods keeps the hood in place and the other one holds the flame arrester on top of the pallet.

Figure 1 shows a close view of the safety valve gate in which the pallet is seated on the valve seat. When the valve is closed, the contact surface of the fluid with the pallet is smaller than when the valve is open.

2.1.1 Material selection. According to the Elmac Technologies website, different materials can be selected for each part, regarding the type of working environment and its working fluid (Table I) (Elmac technologies, 2011).
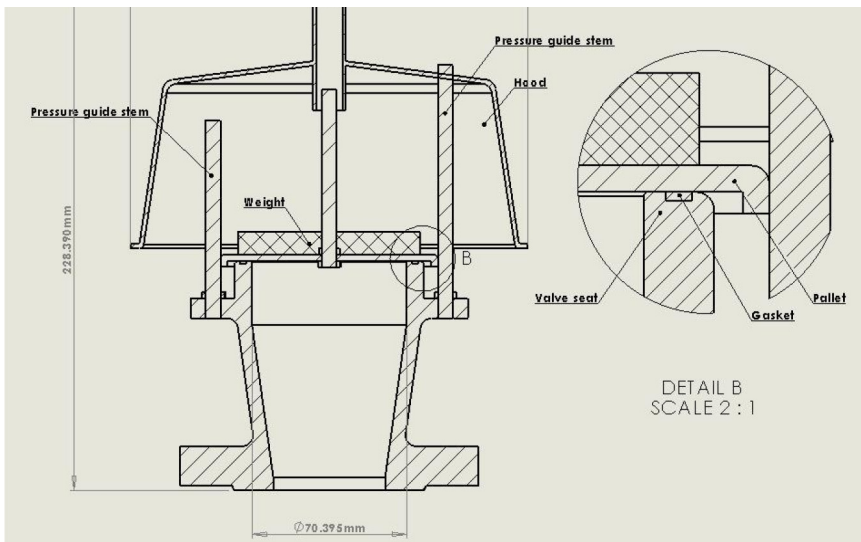
Figure 1. The original design

Table I. List of materials in the original design

Part	Description	Material
1	Valve body	Aluminium, castiron, carbon steel and stainless steel
2	Hood	Aluminium, carbon steel and stainless steel
3	Weight	Lead and stainless steel
4	Pallet	Aluminium and stainless steel
5	Pressure guidepost	Stainless steel
6	O-ring	PTFE, Viton and nitrile rubber
7	Middle rod	Stainless steel

Note: PTFE = Polytetrafluoroethylene

2.2 New design

It is noticeable that the design of weight loaded pressure relief valve is quite simple and changes in this design will most likely make it more complicated. The methods other than weights, such as using magnet based safety valves and duck valves such as the valves used in footballs. These types of safety valves change the force applied on the fluid as function of the valve opening distance. This is because of the fact that magnetic and elastic forces are influenced by the distances over which they act. This effect could cause premature closure of the safety valve. Weight, on the other hand, is only related to mass and gravity, which is almost constant everywhere on earth. It is, therefore, preferable that the new design uses the same concept as weight loaded pressure relief valves. We, therefore, propose a new design on two separate pressure relieving pallets with different sizes and a locking mechanism, which is triggered when overpressure occurs.

2.2.1 Small pallet. The small pallet (Figure 2) serves as an indicator, which moves when the pressure of the tank exceeds a predetermined value. The contact surface of the fluid with the pallet is 3,890 mm² in the old design when the valve is closed. However, this area is reduced to 78.53 mm² in the newly proposed design, which is 50 times smaller than the original design. This change in area means that the force required to open the valve only has to be 50 times smaller than before. The weight placed on top of the pallet is designed to keep the valve closed until the pressure in the tank exceeds 1.08 atmospheres. The weight on top of the fluid is 3.21 kg in the original design. However, in the new design, it becomes as low as 64 g, which is 50 times less than originally.

A rod is also attached to the pallet, which is surrounded by an extension from the hood. This constrains the pallet to move vertically and not to deviate from its path. There is also an extension attached to the pallet, which is examined in the triggering section.

2.2.2 Large pallet. This component (Figure 3) is designed to increase the relief flow of the safety valve. There is no weight located on top of the large pallet, as it is locked in place until it becomes unlocked. The large pallet is designed to use the maximum possible area of the valve gate. It is designed to have 3,000 mm² of contact surface with the fluid when the valve is closed. This value is quite close to the corresponding area for the old design, which is 3,890 mm².

A rod is attached to this pallet similar to that for the small pallet. There is also an extension attached on top of the large pallet, which contains a spring and a bullet attached to the spring.

2.2.3 Locking mechanism. The locking mechanism performs the duty of holding the large pallet in place while fluid pressure is applying force to the bottom of the large pallet.
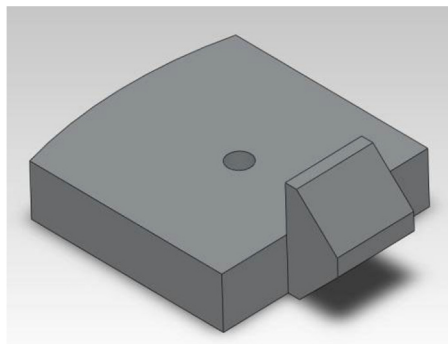
Figure 2. Small pallet

The maximum force that the locking mechanism has to withstand is 22.6 N. This force is equivalent to the force applied to the large pallet by the fluid (which is 24.318 N) after subtracting the weight of the pallet and its extensions (which is 1.71 N).

Figure 4 illustrates the locking mechanism with all of its associated components. As it can be seen in the figure, there is an extension integrated into the top of the large pallet, which houses a spring and the bullet.

2.2.4 Triggering mechanism. The triggering mechanism is designed to unlock the locking mechanism to allow the large pallet to move upwards and relieve the overpressure. As explained in Section 2.2.1, the small pallet would move upwards as soon as the pressure goes beyond 1.08 atmospheres. As it can be seen in Figure 5, there is an extension on the right side of the small pallet, which serves to trigger the locking mechanism. The red circle illustrates the part where the extension from the small pallet touches the bullet.

Upward motion of the small pallet forces the extension to push the bullet inside the locking column while the small pallet passes by the bullet. This exposes the spherical part of the bullet to the inclined hole from the locking column. In this state, the upward force of the fluid overcomes the frictional force of the bullet generated by the spring pushing the bullet, hence, causing the large pallet to move upward to relief the overpressure.

2.2.5 Gasket. There are two gaskets used in this design. One is for the small pallet and the other is for the large pallet. These gaskets are made of rubber and are dimensioned to cause a 1-5 per cent interference. They are used to seal the perimeters around both pallets. The gaskets are always under normal force from both pallets, as they slightly extend vertically beyond the seats. Both pallets are deformed by fractions of a millimetre at
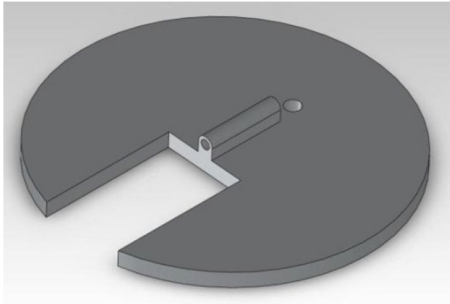
Figure 3. Bigger pallet
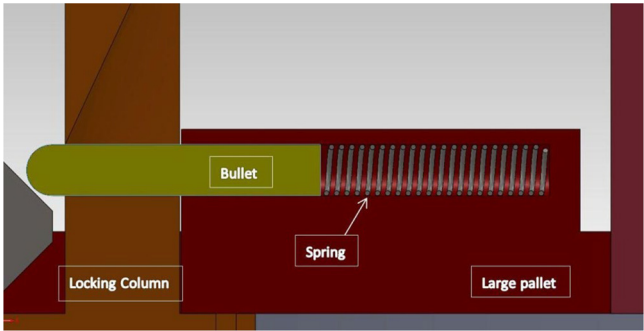
Figure 4. The locking mechanism

maximum fluid pressure. Fluid leakage is prevented by positioning the two gaskets properly.

2.2.6 Hood. The hood (Figure 6) is designed according to the same principles as for the original design. The only difference is that instead of one extension, there are two extensions to keep both stems from the pallets in place and constrain the stem movement to vertical motion. As previously discussed it also prevents intrusion of dust particles and to protects the valve from direct sunlight.

2.2.7 Design overview. Figure 7 illustrates the details of the final design of the safety valve. All the components are marked on the figure for further information.

3. Analysis
3.1 Material selection
Selecting a proper material has a significant effect on the design (Hoseinzadeh and Azadi, 2017; Sohani *et al.*, 2019; Sohani *et al.*, 2016; Yousef Nezhad and Hoseinzadeh, 2017; Hoseinzadeh, 2019; Hoseinzadeh *et al.*, 2019b). Regarding the usage of each part in the design, different materials based on their properties can be selected. Iron-based materials are lower in density compared to lead but are abundant. As high density and low cost are important in choosing a suitable material for the weight in the new design,
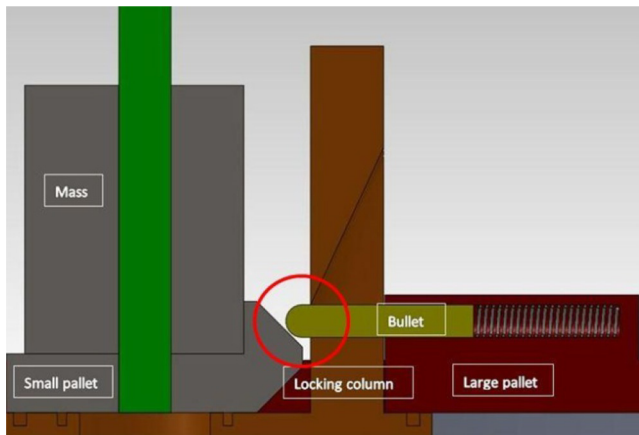
Figure 5. Triggering mechanism
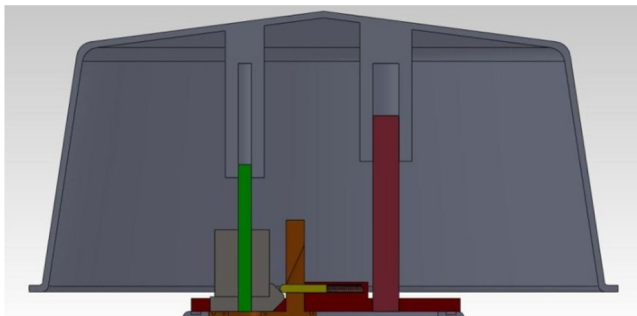
Figure 6. The hood
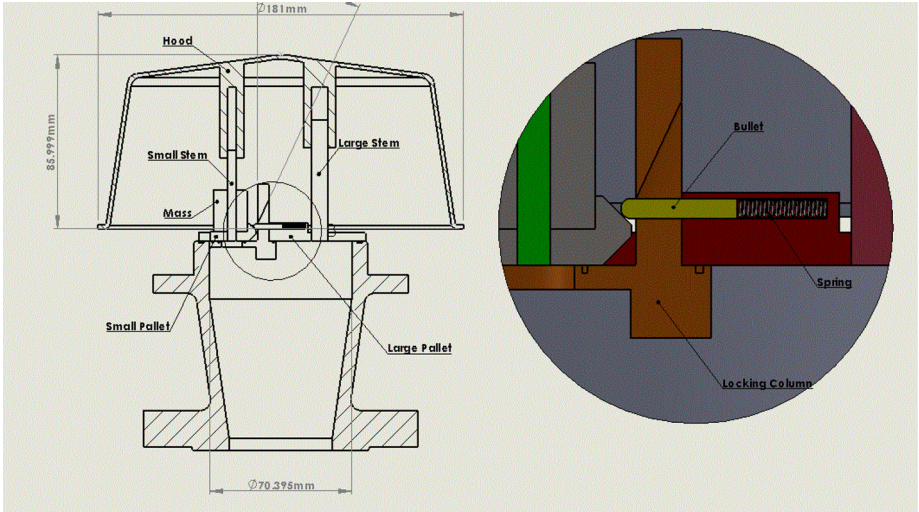
Figure 7. The overview of the new design

the best option is cast iron. In this case, creating the required weight is the main objective; and because of the simple geometry of the weight the machinability does not play an important role.

Other parts in the design have to tolerate exposure to high stresses, especially when the fluid pressure is reaching the pressure limit (Yari *et al.*, 2014; Chamkha, 1994). To overcome this and prevent plastic deformation, the yield strength is an important mechanical property that has to be taken into account. Also, the corrosion resistance and resistance to acids should be as high as possible to prevent friction between moving parts. Considering these requirements, CES EduPack 2011 was used to identify AISI 440 stainless steel as the most appropriate choice at the lowest price available.

3.2 Finite element analysis

A finite element analysis (FEA) was subsequently conducted for the three-dimensional model shown in Figure 8, using the Solidworks 2011 software (Figure 8). The effect of the maximum force that could be applied by the fluid was to be studied to determine the capability of this design to tolerate this force. The system is considered just before the locking mechanism is triggered. Thus, everything is in its initial state.

With the material selected as discussed above, and considering the degrees of freedom of each part, boundary conditions were set as follows:

- The base part is fixed from its right side, assuming that this side can be considered as one with the valve body, so that it cannot move.
- Movement of both discs are restricted to upward motion.
- The relation between the bullet and the column is defined with a pin connection with translation and no rotation inside the column.
- An external pressure of 8,106 Pa is applied to the bottom surfaces of the pallets.

7

3.3 Computational fluid dynamics analysis

In this investigation the ANSYS CFX software was used to study the behaviour of fluid flow through the safety valve because the software is capable of using a dynamic mesh to simulate flows that move through the moving parts (Hoseinzadeh *et al.*, 2019a; Hoseinzadeh *et al.*, 2017; Sudarsana Reddy and Chamkha, 2017; Mansour *et al.*, 2014; Erfan Khodabandeh *et al.*, 2019; Selimefendigil and Chamkha, 2019; Goodarzi *et al.*, 2019; Goodarzi *et al.*, 2014). The calculations are based on the second-order backward Euler scheme for the transient flow (Wakif *et al.*, 2016; Wakif *et al.*, 2017; Wakif *et al.*, 2018b; Wakif *et al.*, 2018a; Wakif *et al.*, 2018c; Wakif, 2019; Hoseinzadeh *et al.*, 2019a; Hoseinzadeh *et al.*, 2019c; Hoseinzadeh *et al.*, 2019d).

A two-dimensional geometry of the current design with true dimensions was drawn and meshed in ANSYS Workbench environment. The ANSYS CFX software consists of three parts: CFX-pre, CFX-solver and CFX-post. The geometry was imported into CFX-pre.

To enhance the results, the quality and quantity of the mesh were also studied. In this analysis, a quadratic mesh was selected because of its higher accuracy compared to a triangular mesh (Yari *et al.*, 2015; Kohzadi *et al.*, 2018). Figure 9(a) shows a row of stretched mesh between the pallet and the valve seat. To prevent this problem, the distance between these parts was filled with more than five rows of mesh cells
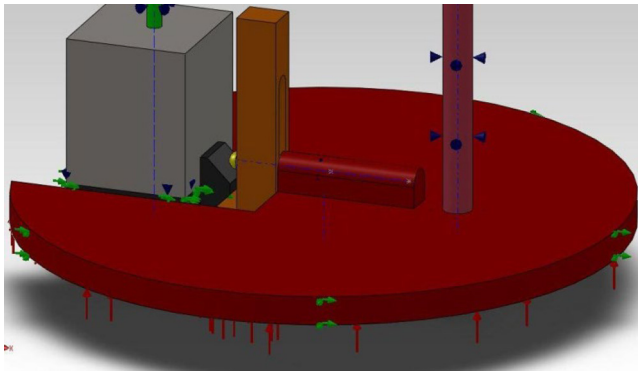
Figure 8. Boundary conditions for the new design
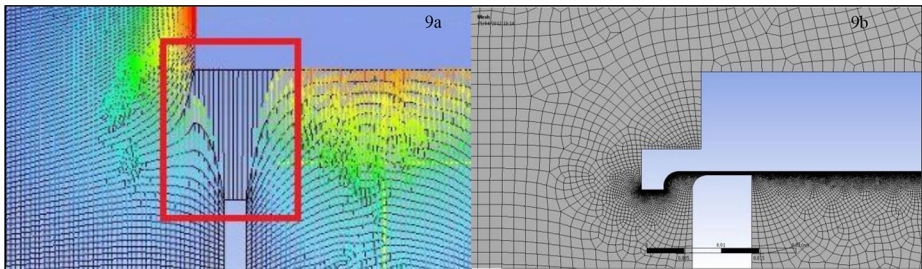
Figure 9. (a, b). The meshing of the valve

[Figure 9(b)]. As we know, the smallest possible distance with the highest mesh density must be provided. In this case, the distance between the pallet and valve seats is 0.2 mm.

3.3.1 CFX-solver. The meshed geometry was subsequently imported to assign the boundary conditions and prepare it for simulation as follows:

The inlet pressure was set to be 1.08 Pa. Methane with a temperature of 298°C was considered as the working fluid. The buoyancy model comprised the application of a gravity force, typically applied to fluid in simulations of heat transfer problems, in which the warmer gas will move above the fluid. This was used in the modelling of the safety valve to obtain more accurate results.

An opening boundary condition was applied at the outlet because of the hood above the valve, which is open to the atmosphere so that during the process, both air and fluid can flow beneath the hood.

Figure 10 depicts the pressure relief valve with inlet flow from its bottom, which is shown by grey arrows. The blue arrows illustrate the opening boundary condition in the outlet pressure from both sides.

4. Results and discussion

4.1 Pressure analysis

The pressure contours display the original weight loaded safety valve just before it opens and when it is completely open. In Figure 11(a), the inlet pressure is 109,300 Pa, which is the predetermined pressure limit. However, it has an increasing trend while it reaches the weight, which can be seen as layers of different colour ranges from orange to red. The maximum normal pressure just under the valve is 111,000 Pa. However, the blue region between the weight and valve seat shows that the pressure is below the ambient pressure. This is because of the distance between these two and as it was explained before, this distance is created solely for meshing. Moreover, as the region
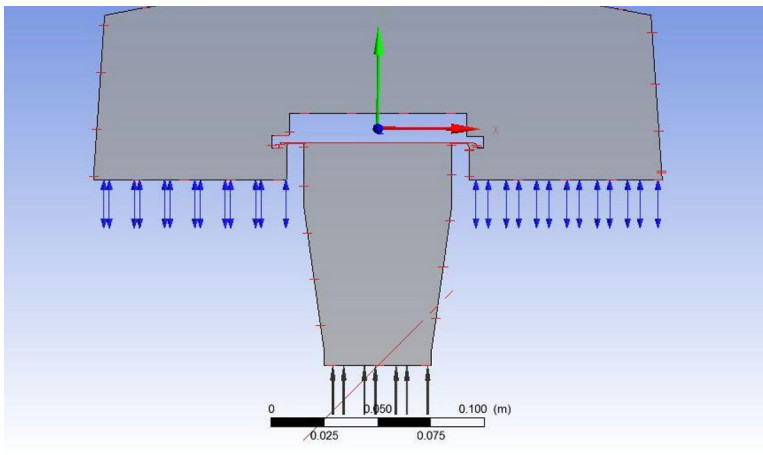
Figure 10. Boundary conditions for the safety valve

9
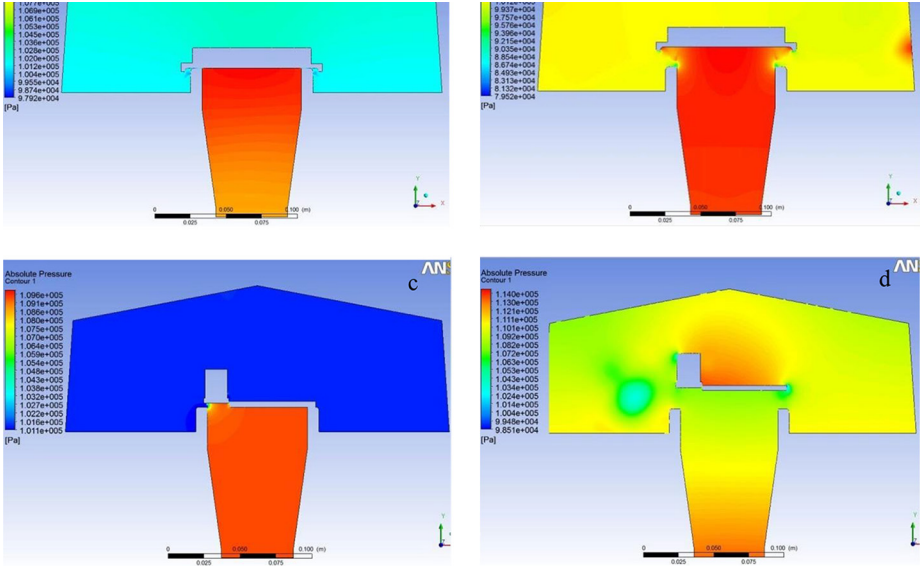
Figure 11. (a, b, c, d). Pressure counters

under the hood is at ambient conditions, the pressure of this region is equal to atmospheric pressure, which is 101,200 Pa.

When the valve is fully open, the pressure inside the hood becomes greater than ambient pressure and reaches up to 103,000 Pa. At this stage, the valve has completely relieved the excess pressure and the pressure inside the valve reaches 109,000 Pa that is 300 Pa smaller than the inlet pressure. Thus, it begins to return on the valve seat.

On the other hand, simulations for the new design show that when the small pallet opens because of small mass flow rate the pressure under the hood is stayed in the atmospheric pressure (the blue region in Figure 11(b). Also, the fluid inside the valve is still dealing with the overpressure with almost the same pressure as the original design in its initial state. Beneath the small pallet in the valve, pressure has divided into three layers of different pressure values. This illustrates that this pressure has decreasing trend while the fluid is approaching the gate and leaving it. In this step, the bigger pallet will be triggered.

In Figure 11(c) the safety valve is releasing the build-up pressure while pallets are lifting. Most of the valve has the pressure of 111,000 Pa, which shows the excess pressure is separated all over the hood. The blue and green regions under the hood present the pressure near to the atmospheric pressure. Moreover, the red colour above the pallets displays that these parts are applying pressure to their fluid above them to be able to move upward [Figure 11(d)].

4.2 Velocity analysis
According to Figure 12 the maximum velocity happens beneath the weight at the fillets with the amount of about 200 m/s. However, the green and yellow regions show that the fluid

10

with the velocity of 105 m/s is entering the atmosphere and the velocity of fluid inside the valve has a velocity of about 60 m/s. As it can be seen, the fluid indicated with blue colour, flows with a negligible amount of velocity around the corners and exactly beneath the weight.

Moreover, the new design has almost the same velocity range as the original design. The same velocity of fluid flows under the hood (the blue regions) but it has a higher velocity around the pallets with the amount of 103 m/s. Moreover, the maximum fluid velocity of 160 m/s has happened besides the small pallet and both sides of these pallets are suffering from turbulences around them.

Because of the distance generated between the pallets with the aim of meshing, the green region with a velocity of 110 m/s is created above them.

4.3 Stress analysis

Figure 13 illustrates the displacement of the pressure relief mechanism just before the valve starts to open. Stainless steel is selected for this analysis because of its high yield strength. The maximum displacement with a negligible amount of 0.00127 mm has happened on the free side of the bigger disc. However, even the smallest displacements can cause flow in the design but existence of the gasket in between the bigger disc and the valve's body will prevent the leakage.

Figure 13 shows stress applied to the parts under this pressure. The maximum stress is 6 MPa and is exerted to the smaller disc where the guide stem meets this disc.
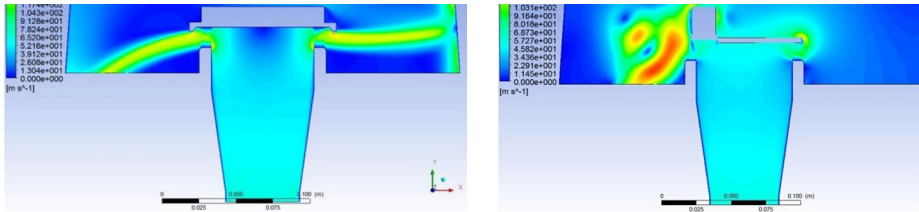
Figure 12. Velocity counters
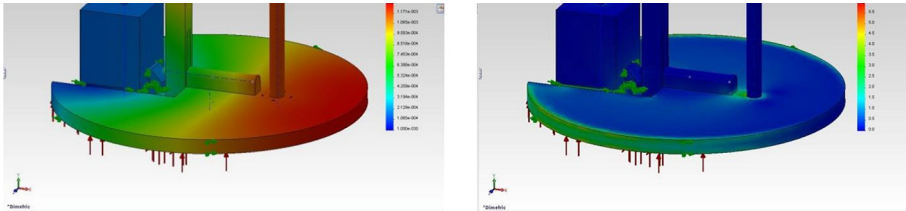
Figure 13. Stress counters

5. Conclusion

This research has tried to develop an enhanced design for pressure relief valve to replace lead with an environmentally friendly material by keeping the general outer dimensions of the design, constant. Moreover, FEA and CFD analysis are carried out to determine the ability of the new design to perform its duty under the same conditions. Results showed that this design can have almost the same performance relative to the original design in relieving the excess pressure.

References

Baladeh, A.E., Cheraghi, M. and Khakzad, N. (2019), "A multi-objective model to optimal selection of safety measures in oil and gas facilities", *Process Safety and Environmental Protection*, Vol. 125, pp. 71-82.

BS EN ISO 4126-1 (2004), "BS EN ISO 4126-1 safety devices for protection against excessive pressure: part 1: safety valves", The European standard, pp. P1-P40.

Bukowski, J.V., Gross, R.E. and Goble, W.M. (2014), "Investigation of adhesion formation in new stainless steel trim spring operated pressure relief valves", *Journal of Pressure Vessel Technology*, Vol. 136 No. 6, p. 61602.

Chamkha, J. (1994), "Unsteady flow of a dusty conducting fluid through a pipe", *Mechanics Research Communications*, Vol. 21 No. 3, pp. 281-288.

Chung, P.W.H., Yang, S.H. and He, C.H. (2000), "Conceptual design of pressure relief systems", *Journal of Loss Prevention in the Process Industries*, Vol. 13 No. 6, pp. 519-526.

Dasgupta, K. and Karmakar, R. (2002), "Dynamic analysis of pilot operated pressure relief valve", *Simulation Modelling Practice and Theory*, Vol. 10 Nos 1/2, pp. 35-49.

Elmac technologies (2011), "Pressure relief valve to atmosphere", Elmac technologies, available at: www.elmactechnologies.com/products/pvrv-381.html (accessed 25 February 2011).

Erfan Khodabandeh, D., Toghraie, A., Chamkha, R., Mashayekhi, O., Akbari, S.A. and Rozati, (2019), "Energy saving with using of elliptic pillows in turbulent flow of two-phase water-silver nanofluid in a spiral heat exchanger", *International Journal of Numerical Methods for Heat and Fluid Flow*, available at: https://doi.org/10.1108/HFF-10-2018-0594

Goodarzi, M., Safaei, M.R., Vafai, K., Ahmadi, G., Dahari, M., Kazi, S.N. and Jomhari, N. (2014), "Investigation of nanofluid mixed convection in a shallow cavity using a two-phase mixture model", *International Journal of Thermal Sciences*, Vol. 75, pp. 204-220.

Goodarzi, M., Tlili, I., Tian, Z. and Safaei, M. (2019), "Efficiency assessment of using graphene nanoplatelets-silver/water nanofluids in microchannel heat sinks with different cross-sections for electronics cooling", *International Journal of Numerical Methods for Heat and Fluid Flow*, available at: https://doi.org/10.1108/HFF-12-2018-0730

Hellemans, M. (2011), "The safety relief valve handbook (2009)", *Process Safety Progress*, Vol. 30 No. 1, pp. 97-98.

Hos, C.J., Champneys, A.R., Paul, K. and McNeely, M. (2014), "Dynamic behavior of direct spring loaded pressure relief valves in gas service: model development, measurements and instability mechanisms", *Journal of Loss Prevention in the Process Industries*, Vol. 31 No. 1, pp. 70-81.

Hoseinzadeh, S. (2019), "Evaluation of a smart window with (WO3+Ag) nanocomposite assisted cooling system on energy saving", *Micro and Nanosystems*, Vol. 11.

Hoseinzadeh, S. and Azadi, R. (2017), "Simulation and optimization of a solar-assisted heating and cooling system for a house in Northern of Iran", *Journal of Renewable and Sustainable Energy*, Vol. 9, doi: 10.1063/1.5000288.

Hoseinzadeh, S., Heyns, P.S. and Kariman, H. (2019a), "Numerical investigation of heat transfer of laminar and turbulent pulsating Al2O3/water nanofluid flow", *International Journal of*

Numerical Methods for Heat and Fluid Flow, available at: https://doi.org/10.1108/HFF-06-2019-0485

Hoseinzadeh, S., Hadi Zakeri, M., Shirkhani, A. and Chamkha, A.J. (2019b), "Analysis of energy consumption improvements of a zero-energy building in a humid mountainous area", *Journal of Renewable and Sustainable Energy*, Vol. 11 No. 1, doi: 10.1063/1.5046512.

Hoseinzadeh, S., Heyns, P.S., Chamkha, A.J. and Shirkhani, A. (2019c), "Thermal analysis of porous fins enclosure with the comparison of analytical and numerical methods", *Journal of Thermal Analysis and Calorimetry*, doi: 10.1007/s10973-019-08203-x.

Hoseinzadeh, S., Moafi, A., Shirkhani, A. and Chamkha, A.J. (2019d), "Numerical validation heat transfer of rectangular cross-section porous fins", *Journal of Thermophysics and Heat Transfer*, pp. 1-7.

Hoseinzadeh, S., Sahebi, S.A.R., Ghasemiasl, R. and Majidian, A.R. (2017), "Experimental analysis to improving thermosyphon (TPCT) thermal efficiency using nanoparticles/based fluids (water)", *European Physical Journal Plus*, Vol. 132.

Kale, S.S. (2014), "Quality assurance and quality control of pressure relief systems", *Process Safety Progress*, Vol. 33 No. 2, pp. 136-142.

Kohzadi, H., Shadaram, A. and Hoseinzadeh, S. (2018), "Improvement of the centrifugal pump performance by restricting the cavitation phenomenon", *Chemical Engineering Transactions*, Vol. 71, pp. 1369-1374.

Mansour, M.A., Bakeir, M.A. and Chamkha, A. (2014), "Natural convection inside a C-shaped nanofluid-filled enclosure with localized heat sources", *International Journal of Numerical Methods for Heat and Fluid Flow*, Vol. 24 No. 8, pp. 1954-1978, available at: https://doi.org/10.1108/HFF-06-2013-0198

Mitchell, E.M., Gross, R.E. and Harris, S.P. (2013), "Evaluating risk and safety integrity levels for pressure relief valves through probabilistic modeling", *Journal of Pressure Vessel Technology*, Vol. 135 No. 2, p. 21601.

Selimefendigil, F. and Chamkha, A.J. (2019), "MHD mixed convection of nanofluid in a three-dimensional vented cavity with surface corrugation and inner rotating cylinder", *International Journal of Numerical Methods for Heat and Fluid Flow*, available at: https://doi.org/10.1108/HFF-10-2018-0566

Sohani, A., Sayyaadi, H. and Hoseinpoori, S. (2016), "Modeling and multi-objective optimization of an M-cycle cross-flow indirect evaporative cooler using the GMDH type neural network", *International Journal of Refrigeration*, Vol. 69, pp. 186-204.

Sohani, A., Sayyaadi, H. and Zeraatpisheh, M. (2019), "Optimization strategy by a general approach to enhance improving potential of dew-point evaporative coolers", *Energy Conversion and Management*, Vol. 188, pp. 177-213.

Srivastava, A. and Gupta, J.P. (2010), "New methodologies for security risk assessment of oil and gas industry", *Process Safety and Environmental Protection*, Vol. 88 No. 6, pp. 407-412.

Sudarsana Reddy, P. and Chamkha, A. (2017), "Heat and mass transfer analysis in natural convection flow of nanofluid over a vertical cone with chemical reaction", *International Journal of Numerical Methods for Heat and Fluid Flow*, Vol. 27 No. 1, pp. 2-22, available at: https://doi.org/10.1108/HFF-10-2015-0412

Wakif, A., Boulahia, Z. and Sehaqui, R. (2016), "Numerical study of the onset of convection in a Newtonian nanofluid layer with spatially uniform and non uniform internal heating", *Journal of Nanofluids*, Vol. 6 No. 1, pp. 136-148.

Wakif, A., Boulahia, Z. and Sehaqui, R. (2017), "Numerical analysis of the onset of longitudinal convective rolls in a porous medium saturated by an electrically conducting nanofluid in the presence of an external magnetic field", *Results in Physics*, Vol. 7, pp. 2134-2152.

Wakif, A., Boulahia, Z. and Sehaqui, R. (2018a), "A semi-analytical analysis of electro-thermo-hydrodynamic stability in dielectric nanofluids using Buongiorno's mathematical model together with more realistic boundary conditions", *Results in Physics*, Vol. 9, pp. 1438-1454.

Wakif, A., Boulahia, Z., Ali, F., Eid, M.R. and Sehaqui, R. (2018b), "Numerical analysis of the unsteady natural convection MHD Couette nanofluid flow in the presence of thermal radiation using single and Two-Phase nanofluid models for Cu–water nanofluids", *International Journal of Applied and Computational Mathematics*, Vol. 4 No. 3.

Wakif, A., Z., Boulahia, S.R., Mishra, M., M., Rashidi, R. and Sehaqui, (2018c), "Influence of a uniform transverse magnetic field on the thermo-hydrodynamic stability in water-based nanofluids with metallic nanoparticles using the generalized Buongiorno's mathematical model", *European Physical Journal Plus*, Vol. 133.

Wakif, A., Boulahia, Z., Amine, A., Animasaun, I.L., Afridi, M.I., Qasim, M. and Sehaqui, R. (2019), "Magneto-convection of alumina – water nanofluid within thin horizontal layers using the revised generalized Buongiorno's model", *Frontiers in Heat and Mass Transfer*, Vol. 12, doi: 10.5098/hmt.12.3.

Wang, J., Weaver, D.S. and Tullis, S. (2012), "Simplified fluid-structure model for duckbill valve flow", *Journal of Pressure Vessel Technology*, Vol. 134 No. 4, p. 41301.

Yari, A., Hosseinzadeh, S. and Galogahi, M.R. (2014), "Two-dimensional numerical simulation of the combined heat transfer in channel flow", *International Journal of Recent Advances in Mechanical Engineering*, Vol. 3 No. 3, pp. 55-67.

Yari, S. Hosseinzadeh, A.A. Golneshan, R. and Ghasemiasl, (2015), "Numerical simulation for thermal design of a gas water heater with turbulent combined convection", ASME International, p. V001T03A007, available at: https://doi.org/10.1115/ajkfluids2015-3305

Ye, Q. and Chen, J. (2009), "Dynamic analysis of a pilot-operated two-stage solenoid valve used in pneumatic system", *Simulation Modelling Practice and Theory*, Vol. 17 No. 5, pp. 794-816.

Yousef Nezhad, M.E. and Hoseinzadeh, S. (2017), "Mathematical modelling and simulation of a solar water heater for an aviculture unit using MATLAB/SIMULINK", *Journal of Renewable and Sustainable Energy*, Vol. 9 No. 6, doi: 10.1063/1.5010828.